

Nematic and Cholesteric Thermotropic Polyesters with Azoxybenzene Mesogenic Units and Flexible Spacers in the Main Chain

A. BLUMSTEIN, S. VILASAGAR, S. PONRATHNAM, S. B. CLOUGH, and R. B. BLUMSTEIN, *Department of Chemistry, Polymer Science Program, University of Lowell, Lowell, Massachusetts 01854* and G. MARET, *Hochfeld Magnet Labor, Max Planck Institut fuer Festkörperforschung, F-38042, Grenoble Cedex, France*

Synopsis

Properties of linear polyesters based on azoxybenzene and 2,2'-methylazoxybenzene moieties with linear, flexible spacers based on mixtures of dodecanedioic acid (DDA) and methyladipic acid (MAA), chiral or racemic, of various compositions (system MAA/DDA-8 and MAA/DDA-9, respectively) have been described. Substitution of methyl groups in the 2,2' or 3,3' positions of the mesogenic core leads to soluble and relatively low-melting-point polyesters. The viscosity law for (MAA/DDA-9) polyesters in 1,1,2,2 tetrachloroethane gives an exponent 0.76, indicating well-solvated, coiled chain conformations in dilute solution. Calorimetric data show an increase in isotropization entropy ΔS_{NI} with increasing average length of the spacer. This suggests a nonrandom conformation of the spacer in the nematic melt with a degree of order superior to that of low-molecular-weight analogs. X-ray data obtained with an oriented nematic glass quenched from the nematic melt of DDA-9 subjected to a magnetic field of 10–12 T also support the extended-chain model in the nematic phase of DDA-9. Oriented fibers can be produced by subjecting nematic melts of polyesters 8 and 9 either to magnetic fields of high intensity or to shear fields. The x-ray data obtained from these fibers also support the extended-chain model. Cholesteric systems do not orient in the magnetic field of 10–12 T. The study of mesophases of systems 8 and 9 indicates a dramatic influence of the position of the ester group on the stability of the mesophase in the azoxybenzene polyesters. The results are interpreted in terms of geometric factors influencing the colinearity of the mesogenic core and of the extended spacer.

INTRODUCTION

We have recently described^{1,2} the synthesis and properties of some linear smectic, nematic, and cholesteric thermotropic polyesters and a number of papers have also appeared in the literature,^{4–10} describing similar systems. As synthesis progresses in various laboratories, structure-property correlations for thermotropic linear polymers are slowly emerging. Mesophase characterization is usually based on techniques such as x-ray diffraction, polarizing microscopy, differential scanning calorimetry, and other methods commonly used for identification of low-molecular-weight liquid crystals. Criteria for structural classification developed for low-molecular-weight mesophases do not always unequivocally apply to polymers and positive identification of the polymeric mesophase may be difficult. Because of high viscosity, broad molecular weight distributions, and the coexistence of polycrystalline and amorphous material, microscopic observation of specific textures can be misleading. Differential scanning calorimetry (DSC) is complicated by the same factors, and interpre-

tation of DSC traces is much more difficult for mesomorphic polymers than for the corresponding low-molecular-weight liquid crystals.

X-ray patterns may be of help in the case of smectic mesophases. They are, however, often too diffuse to be used for unoriented nematic or cholesteric phases. A need exists, therefore, to synthesize polymers with unambiguous mesophase behavior. We have found that polyesters based on the azoxybenzene mesogenic moiety give such thermotropic phases with textures clearly characteristic of nematic and cholesteric phases.^{2,3} In this paper we present studies of structure-property correlations for such polyesters.

EXPERIMENTAL

In Table I are presented the various moieties and flexible spacers used in this study. Synthesis of the mesogenic moieties 8 and 9 was conducted according to procedures described in the literature.^{11,12} The acid chlorides were prepared from corresponding acids with thionyl chloride; the corresponding diols were obtained from commercial sources. The polyesterification was carried out either in 1,2-dichloroethane solution or by interfacial polycondensation by condensing the sodium salt of the diphenol with the acid chloride at the water-dichloroethane interface.^{1,2} The 4,4'-azoxybenzoic acid chloride was prepared according to the procedure described in ref. 13. The polyesterification was carried out in dry chloroform in the presence of dry pyridine. All polymers were precipitated into methanol, washed abundantly with methanol, and dried *in vacuo*.

Elemental analysis agreed well with the calculated values. Textures of polymers were studied between a slide and cover slip using a Leitz Ortholux polarizing microscope equipped with a hot stage and a Mettler FP-52 temperature programmer. The polymers were characterized by their limiting viscosity number at 30°C [in a (1:1 wt) mixture of *m*-cresol and chloroform, in 1,1,2,2-tetrachloroethane, or in chloroform] and by the \bar{M}_n determined by vapor pressure osmometry (VPO) in 1,1,2,2-tetrachloroethane or chloroform at 36°C by means of a Knauer VPO osmometer. The thermal properties were investigated by means of a Perkin-Elmer 2-C differential scanning calorimeter.

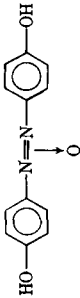

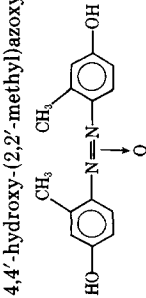
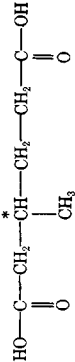
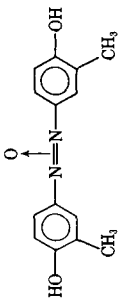
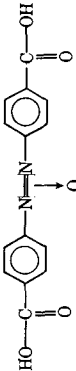
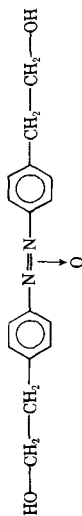

The orientation of polymers DDA-8 and DDA-9 was performed in a magnetic field of 10–16 T. The polymers were heated above their crystal to nematic (K/N) transition temperature and cooled slowly (0.2–1°C/min) to room temperature, while the magnetic field was maintained. In addition, the DDA-9 polymer was oriented by extrusion: the polymer in its nematic state at 136°C was extruded through a die with an orifice of 0.02 in. The fiber was then rapidly drawn and passed through a cooling water bath.

X-ray patterns of oriented and unoriented samples were obtained with a Laue camera using Ni-filtered Cu_α radiation with a sample-to-film distance of 8 cm. A Warhus flat-plate camera was also used. The orientation function f_c was obtained by measuring the azimuthal angular intensity distribution $I(\chi)$ with a Joyce-Loebl microdensitometer. f_c was then calculated by area integration according to

$$\overline{\cos^2\chi} = \int_0^{\pi/2} I(\chi) \cos^2(\chi) \sin(\chi) d\chi / \int_0^{\pi/2} I(\chi) \sin(\chi) d\chi,$$

$$f_c = \frac{1}{2}(3 \overline{\cos^2\theta} - 1)$$

TABLE I
Monomers Used in the Preparation of Azoxy Polyesters^a

Diol or diphenol	Symbol	Diacid	Symbol
<p>4,4'-hydroxyazoxybenzene</p> 	8	<p>decandioic</p> 	DDA
<p>4,4'-hydroxy-(2,2'-methyl)azoxybenzene</p> 	9	<p>3-methyladipic</p> 	MAA* or MAA
<p>4,4'-hydroxy-(3,3'-methyl)azoxybenzene</p> 	14	<p>4,4'-azoxybenzoic</p> 	Azoxy B
<p>4,4'-hydroxyethyloxybenzene</p> 	10	<p>subaric acid</p> 	SUB
HO-(CH2) _n -OH	n-ol		

^a Asterisk designates chirality.

with $\overline{\cos^2\theta} = 1 - 2\overline{\cos^2\chi}$ and with χ the angle between the director and the chain orientation.

RESULTS AND DISCUSSIONS

Dilute-Solution Properties

As we pointed out in a previous paper, the polyester derivatives of azoxybenzene (series 8) spontaneously display typically nematic textures.^{2,3} Some thermal decomposition, however, was observed at the nematic/isotropic (N/I) transition temperature. In order to lower the transition temperatures we synthesized the 2-2'-methyl derivative of 8 (series 9).³ As expected, the polymers in series 9 are characterized by significantly lower transition temperatures and high solubility relative to their series-8 counterparts.

Table II gives the data on limiting viscosity number $[\eta]$ and \overline{M}_n for samples of polyesters of series 9 with mesogenic moieties separated by DDA or MAA spacers or copolymers containing both spacers. The experimental points fit quite well the equation represented by Figure 1:

$$[\eta]^{30^\circ} = 4.65 \times 10^{-4} \overline{M}_n^{0.76}$$

It is interesting to note that this relation is equally well followed by polyesters with various chiral contents and various average spacer lengths. Consequently these polymers appear to be well solvated by chlorinated hydrocarbons and to display coiled conformations in dilute solution, a result which is in agreement with our magnetic birefringence data.¹⁴

Thermal Behavior

Table III gives transition temperatures and enthalpies and entropies of isotropization (ΔH_{NI} and ΔS_{NI}) for MAA*/DDA-9 copolymers of various compositions and average spacer length \bar{n} (the ester group is considered as part of the

TABLE II
Limiting Viscosity Number at 30°C and Molecular Weight of Various MAA-DDA-9 Polyesters^a

Sample	Polymer	Solvent	$[\eta]$ (dl/g)	\overline{M}_n (g/mol)
1	DDA-9	1,1,2,2-tetrachloroethane	0.20	2800
2	MAA*-9	1:1 <i>m</i> -cresol chloroform	0.42	7800
3	MAA*/DDA (50/50)-9	1:1 <i>m</i> -cresol chloroform	0.58	10,800
4	DDA-9	1,1,2,2-tetrachloroethane	0.50	11,500
5	MAA*/DDA (25/75)-9	1:1 <i>m</i> -cresol chloroform	0.60	11,700
6	DDA-9	1,1,2,2-tetrachloroethane	0.69	13,600
7	MAA-9	1,1,2,2-tetrachloroethane	0.74	16,000

^a Asterisk designates chirality.

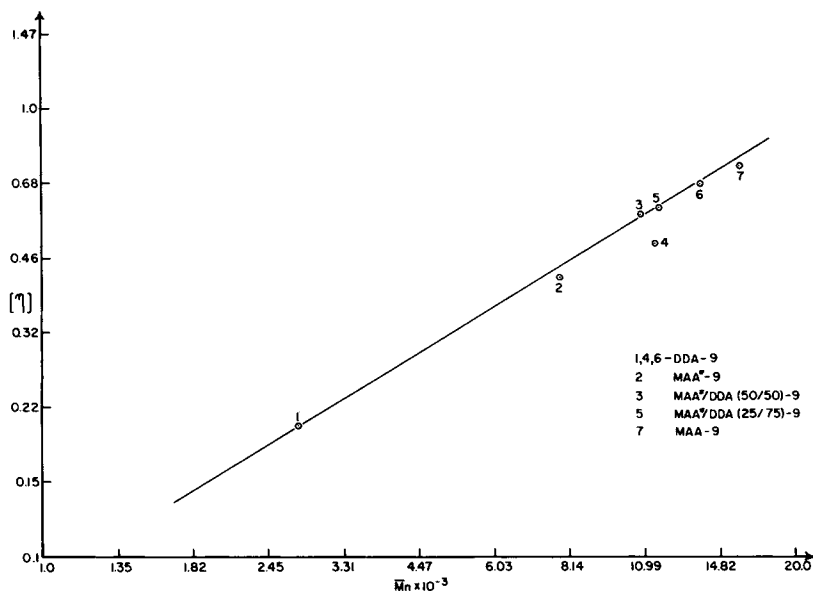


Fig. 1. Limiting viscosity number–molecular weight relationship in DDA/MAA*-9 polyesters in 1,1,2,2-tetrachloroethane.

spacer). The corresponding values of transition temperatures for the series 8 are given in Figure 3(a). Because of high isotropization temperatures impinging on decomposition, no reliable ΔH_{NI} and ΔS_{NI} could be obtained for some copolymers 8 and this series is not included in Table III.

As one can see from Table III, series 9 is characterized by a steady increase

TABLE III
Thermal Properties of the MAA*/DDA-9 System

MAA*/DDA-9 (x/y)	Transition temperature (°C)	\bar{n}	$\frac{\Delta H_{NI}}{(\text{kJ/mru}^a)}$	$\frac{\Delta S_{NI}}{(\text{J/mol})}$	$\frac{\bar{M}_n}{(\text{g/mol})}$
100/0	K151CH201I	8	3.18	6.71	7,800 ^c
75/25	K132CH193I	9.5	3.34	7.19	8,300 ^b
50/50	K76CH178I	11	3.86	8.56	10,800 ^c
25/75	K96CH169I	12.5	4.60	10.41	11,700 ^c
0/100	K118N162.5I	14	5.64	12.95	13,000 ^b

^a mru = mole of repeating unit.

^b Calculated from eq. (1).

^c Measured by VPO.

of ΔS_{NI} with \bar{n} . In addition the values of ΔS_{NI} are two to three times higher than for the corresponding low-molecular-weight *p-n*-alkoxyazoxybenzenes.¹⁵ This indicates a higher degree of order (translational, orientational, or both) in the nematic polyester than in similar nematic low-molecular-weight compounds. This is in agreement with our values of the order parameter in the nematic melt of DDA-9, which we have found to be higher than in the nematic *p*-azoxyanisole (PAA).¹⁶

Influence of Azoxy Polyester Structure on Position and Breadth of Mesomorphic Interval

Table IV gives the transition temperatures of various polyesters, at constant spacer length $n = 14$ (the ester groups are counted as being part of the spacer). When the carbonyl group is adjacent to the benzene ring (azoxy-B-10) the interval between the DSC endotherms is very narrow, some 3°C, and microscopic observation reveals no characteristic mesomorphic texture. In sharp contrast,

removal of the $\begin{array}{c} \text{C} \\ || \\ \text{O} \end{array}$ group one atom away from the benzene ring (by inverting the sequence of ether and carbonyl linkages, as in polymers DDA-8, DDA-9, and DDA-14) dramatically increases the breadth of the mesophase interval, and characteristic mesophase textures are observed (Fig. 2). Further removal of the carbonyl by several atoms from the azoxybenzene moiety again produces a considerable narrowing of the mesophase (SUB-10).

Figures 3(a), 3(b), and 3(c) give the transition temperature and breadth of the mesomorphic interval for copolymer systems MAA*/DDA with mesogenic units 8, 9, and 10, respectively. One can see that the introduction of a methyl group into the mesogenic moiety drastically lowers the transition temperature. However, the breadth of the mesomorphic interval decreases in the case of DDA-14. By incorporating MAA and DDA units in variable proportions, one can also depress substantially the K/N transition, as is apparent from Figures 3(a) and 3(b). The temperature of isotropization appears to be much less affected. This points toward an increased tolerance of the nematic phase for structural differences between various parts of the macromolecule. In MAA/DDA-10 [Fig. 3(c)], containing a flexible spacer with six additional flexible bonds the transition temperatures appear to be less affected than in the series-8 and -9 polyesters.

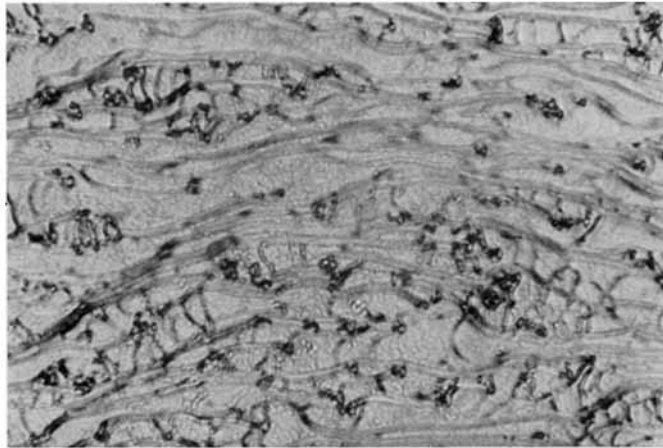
In addition to structural differences in the mesogene and in the flexible spacer, the length of the flexible spacer may also affect the breadth of the mesomorphic interval. For example, in systems 8 and 9 the average spacer length \bar{n} offering the lowest liquid-crystalline mesophase transition temperatures is 8–10 flexible bonds. Spacers which are too long may collapse the mesophase by a simple dilution effect, while short spacers may introduce steric constraints, leading to an unfavorable geometry of the repeating unit.

Influence of Molecular Weight

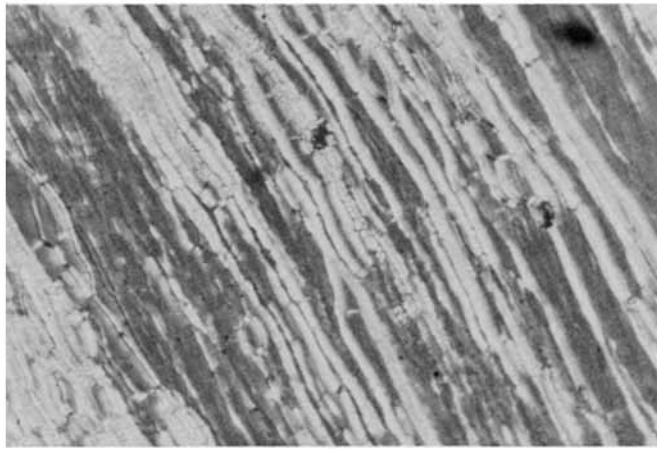
Figure 4 gives the variation of the transition temperatures as a function of the number-average molecular weight of DDA-9 samples. It can be seen from Figure

TABLE IV
Influence of Ester-Group Position on the Mesomorphic Temperature Interval of Azoxy Polyesters

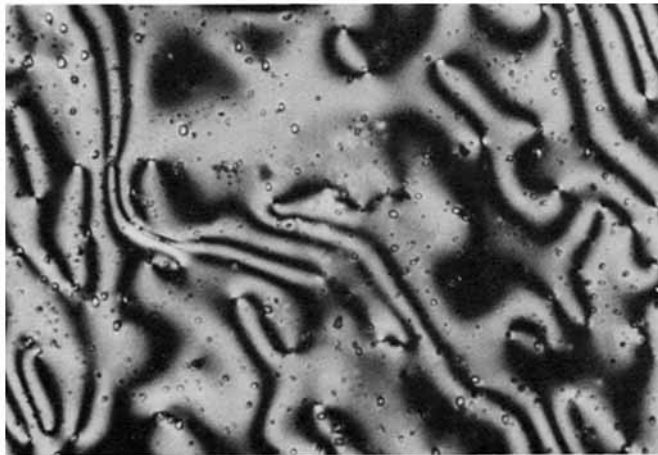
Polymer	Chemical Structure	Transitions (°C)	Δt (°C)	\bar{M}_n (g/mol)
DDA-8		K216N265I	49	16,900
SUB-10		K185; 191I	6	9,700
AzoxyB-10		K198; 201I	3	4,700
DDA-9		K118N162.5I	44.5	13,000
DDA-14		K142N165I	23	15,900



(a)



(b)



(c)

Fig. 2. Oily streak textures of twisted nematic mesophases: (a) MAA*/DDA-(1/1)-8, $\bar{M}_n = 10,800$, 240°C, with green iridescent background; (b) MAA*/DDA-(1/1)-9, $\bar{M}_n = 10,800$, 160°C, with blue iridescent background (ca. 300 \times). (c) Typical nematic "schlieren" texture obtained with DDA-8 $\bar{M}_n \approx 15,000$ at 230°C (ca. 300 \times).

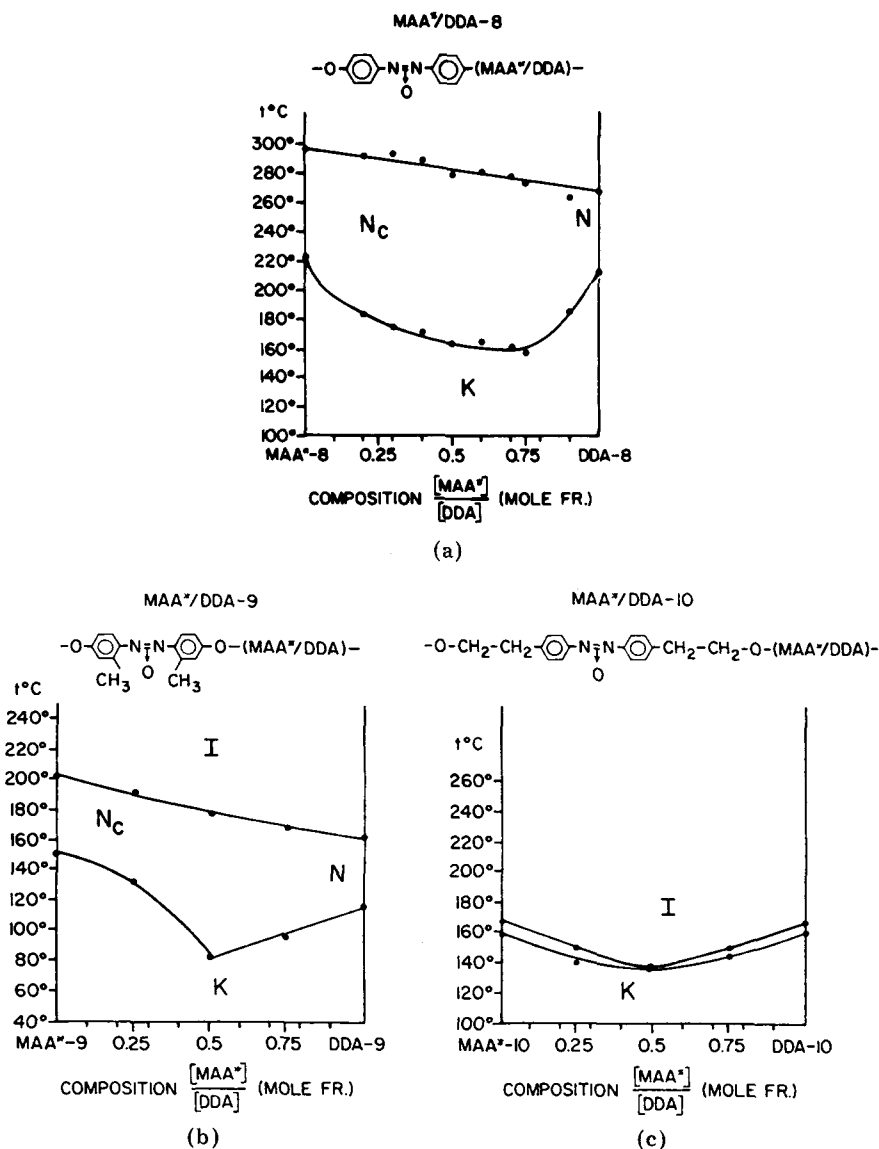


Fig. 3. (a)–(c) Transition temperatures as a function of composition for systems MAA*/DDA 8, 9, and 10, respectively.

4 that both K/N and N/I transitions reach a plateau at \bar{M}_n of approximately 6000–7000. For lower molecular weights, a significant depression of both transition points takes place and the mesomorphic interval narrows rapidly. The exact nature of the transition-temperature dependence for very low molecular weights ($\bar{M}_n < 2000$) is not known with precision at this time. Work is in progress with well-fractionated samples and oligomers to allow a more quantitative determination of the relationship between molecular weight and the transition temperatures.

TRANSITION TEMPERATURES
AS A FUNCTION OF \bar{M}_n FOR THE DDA-9
POLYESTER

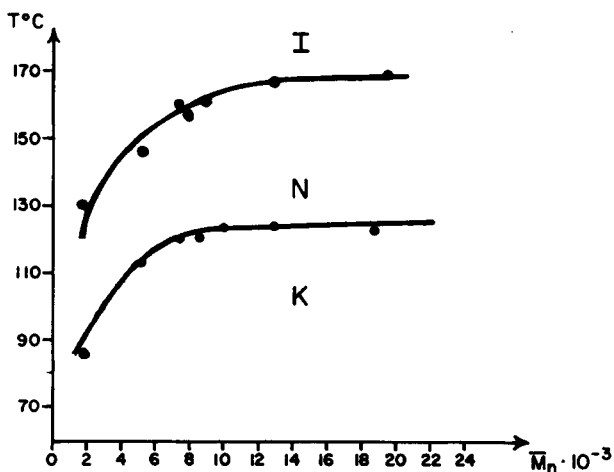
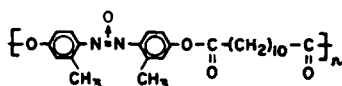


Fig. 4. Dependence of the transition temperatures on \bar{M}_n for DDA-9.

Chirality and Formation of Cholesteric Phases

As we have noted previously, the chiral systems, MAA*/DDA-8² and MAA*/DDA-9³ [where MAA* symbolizes the (+)3-methyladipic acid unit in the flexible spacer] induce cholesteric behavior, characterized by iridescence due to selective reflections of light. We have also indicated that the pitch of the cholesteric helix varies with the increase in the content of the chiral MAA* units. This is in agreement with previous results of Finkelmann¹⁷ for polymers containing mesogenic and chiral elements in the side groups.

Near 230°C the MAA*/DDA-8 system displays a blue iridescence in the 70/30–60/40 composition range. This changes to yellow-green for 50/50 and to orange-red for 40/60 compositions. Other compositions on both sides of this interval give no visible selective reflections but present, under slide and cover glass, the “oily streak” textures characteristic of cholesteric mesophases [see Figs. 2(a) and 2(b)].

The system MAA*/DDA-9 is also iridescent in orange-red for 25/75 and in blue for 50/50 at 140–160°C, and, unlike system 8, the iridescence can be “locked in” by quenching. This could well be due to a slower crystallization of the methyl-substituted mesogene. No iridescence was observed in system 10, in which the nature of the mesophase could not be positively identified owing to its narrow interval [Fig. 3(c)].

Orientation

The orientation of systems 8 and 9 has been achieved by cooling the specimen in a high-intensity magnetic field (12–16 T) from its melted state.^{18,21,22} As has been pointed out recently,^{18,22} the racemic system 8 orients easily in a field of 10–16 T in its nematic state, while the chiral system 8 in its cholesteric state does not orient. Both systems give at room temperature x-ray patterns characteristic of polycrystalline materials. Table V gives representative x-ray data for both systems.

Above the first transition temperature all polymers of both systems gave halos around 4.9–5.3 Å. The absence of a sharp low-angle spacing indicates that the systems are not smectic. It appears from Table V that the DDA component of the flexible spacer has a predominant tendency to crystallize and that the DDA-9 crystal pattern persists beyond the 1:1 (MAA)/(DDA) composition of the spacer.

The spacings for unoriented and oriented specimens of DDA-9 are given in Table VI. The unoriented specimens were annealed at 120°C. The oriented specimens were prepared either by heating the polymer above its N/I transition temperature, applying a field of 12 T, and cooling slowly to room temperature, or by extruding a fiber from the nematic melt (see the Experimental section).

One can see from Table VI that both methods provide a means of orienting

TABLE V
Room-Temperature Spacings for Systems 8 and 9

MAA*/DDA-8	Spacings (Å)
100/0	3.78; 4.30; 4.99 and a series of weaker peaks
50/50	3.72; 4.15; 4.78
0/100	3.42, 4.23; 8.21; 13.2, 15.7
MAA*/DDA-9	
100/0	3.94; 4.95
75/25	3.92; 4.95
50/50	3.70; 4.04; 4.36; 4.59; 7.09 (m), 11.2 (m)
25/75	3.70; 4.06; 4.36; 4.63; 7.09 (s), 11.3 (m)
0/100	3.72; 4.08; 4.38; 4.65; 7.14; 11.5 (s)

TABLE VI
Room-Temperature *d* Spacings (in Å) for DDA-9 after Cooling from the Nematic State

Unoriented (annealed)	Oriented (magnetic field) ^a	Fiber (extrusion) ^b
11.5	11.3 meridian	15.8; 50° from meridian
7.13	6.95 50° from meridian	
4.65	4.61; ~40°	4.62; equator
4.38	4.33; equator	4.25; meridian
4.08	4.06; ~60°	3.89; equator
3.72	3.69; ~60°	
	plus additional weaker lines	
f_c^c	0	0.6 (estimated)
		0.88

^a Specimen $\bar{M}_n \approx 4000$, field ca. 12 T [see Fig. 5(b)].

^b Specimen $\bar{M}_n \approx 20,000$ [see Fig. 5(c)].

^c Orientation function $f_c = \frac{1}{2}(3 \cos^2\theta - 1)$, with θ the angle between the field and the chain orientation from the strongest equatorial reflection.

TABLE VII
Room-Temperature d Spacings (in Å) for DDA-8

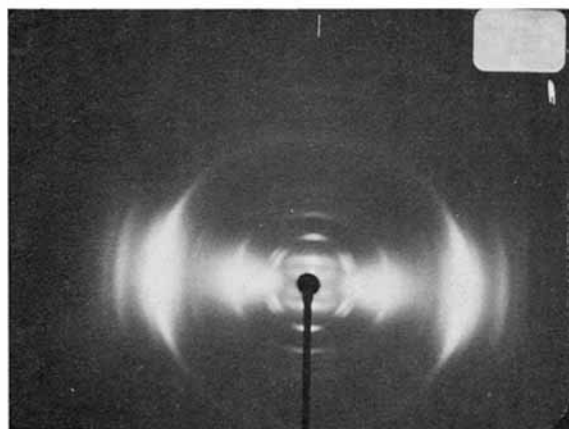
	Unoriented (annealed)	Oriented by magnetic field
	15.7	25.7; meridian
	13.2	15.2; $\sim 55^\circ$ from meridian
		13.1; $\sim 55^\circ$
		12.9; meridian
	8.21	8.96; meridian
		8.13; equator
		6.52; meridian
		5.29; meridian
	4.23 (strong)	4.16; equator(s)
	3.42	3.39; equator
f_c	0	0.93

DDA-9. However, the orientation function f_c of the crystalline sample oriented by the magnetic field is low. In contrast, the orientation function of the extruded fiber is very high. One can see clearly from Figure 6 that DDA-9 in its nematic state displays, when subjected to high magnetic fields, a high degree of orientation. One can therefore conclude that the orientation of DDA-9 is disturbed by crystallization on cooling from the oriented nematic melt, in analogy to several other nematic or potentially nematic polyesters.²²

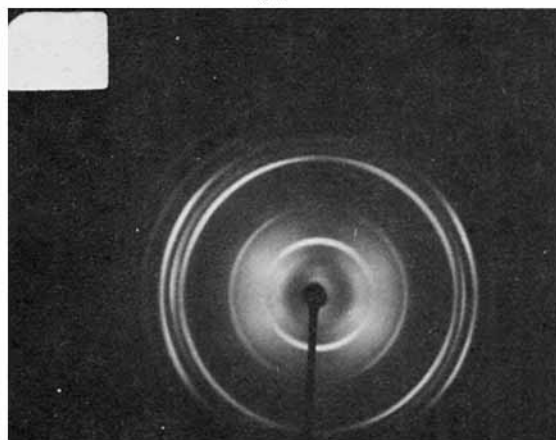
The polymer DDA-8 was also oriented in its nematic state (235°C) by means of a magnetic field of 11 T and cooled at 1°C/min to room temperature [Fig. 5(a)]. A substantially higher orientation ($f_c = 0.93$) was achieved than for DDA-9 even though the molecular weight of the specimen of DDA-8 was substantially higher. The value of f_c was computed from the most intense equatorial peak.

Table VII gives the d spacings of oriented and unoriented DDA-8. Here again, as in DDA-9 the lines from a powder annealed at 180°C have the same spacings as in the oriented specimen though fewer lines were observed. The largest spacing on the meridian is 25.7 Å. It corresponds to the calculated length of the repeat unit of 25.2 Å with a fully extended methylene chain. Other meridional peaks are higher orders of this period. Thus for DDA-8 we envisage crystals with chains extended and aligned with the field and with the mesogenic units stacked in layers normal to the chain direction [Fig. 7(a)].

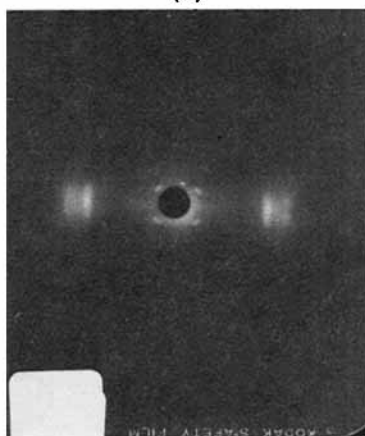
For DDA-9 oriented in the magnetic field (Table VI) the largest meridian reflection corresponds to 11.2 Å, less than half the length of the stretched repeat unit of 25.2 Å. This may possibly be interpreted in terms of a tilt of the repeat unit within the crystallite. Here again as in DDA-8 the unoriented samples and samples oriented by the magnetic field have spacings that appear to be the same and hence correspond to the same basic crystal structure. In contrast the specimen drawn as a fiber [Fig. 5(c) and Table VI] has a different set of lower-angle spacings and hence a crystal structure different from that of the undrawn samples. The 15.8-Å spacing at 50° from the fiber direction suggests the following model [see Fig. 7(b)]: the aliphatic portion of the molecule is extended in the crystals, the mesogenic units are still packed in layers as in DDA-8 [Fig. 7(a)], but the layers are tilted with respect to the fiber axis. The distance along the repeat units for this model, 24.6 Å, compares reasonably well with the calculated length of the fully extended chain of 25.2 Å.



(a)



(b)



(c)

Fig. 5. (a) X-ray photograph, beam normal to H, of a DDA-8 specimen oriented by a field of 11 T at 235°C and cooled in the field to room temperature at 1°C/min ($\bar{M}_n \approx 14,000$ –15,000). (b) X-ray photograph of a DDA-9 specimen oriented by a field of 12 T at 138°C and cooled in the field to room temperature at 0.5°C/min ($\bar{M}_n \approx 3000$ –4000). (c) X-ray photograph, beam normal to the direction of extension of a DDA-9 fiber drawn through a 0.02-in. orifice, at 136°C ($\bar{M}_n \approx 18,000$ –20,000; sample-to-film distance 5.3 cm).

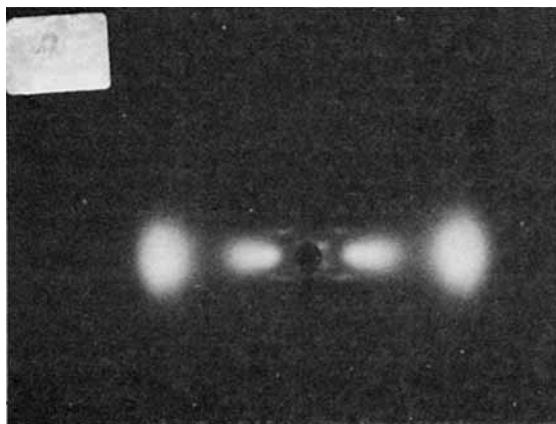


Fig. 6. X-ray photograph of a DDA-9 specimen of Fig. 5(b) quenched at a rate $100^{\circ}\text{C}/\text{min}$.

When DDA-9 was quenched from the oriented nematic state, a nematic glass was obtained. Figure 6 shows the x-ray diffraction pattern, which is quite similar to the pattern of the aligned nematic phase of 4-4'-*n*-alkoxyazoxybenzene obtained by Chistyakov and Chaikovsky¹⁹ with inner and outer-diffuse nematic peaks showing orientation of the chains. The spacing (Bragg equation) of the inner peak at about 51° from the meridian is 16.5 \AA . We envisage a possible cybotactic nematic arrangement²⁰ of chains similar to that in Figure 7(c), but without long-range order. The basis for this assignment is given by deVries,²⁰ who points out that the simplest way to account for the pattern in Figure 6 is to have a bundle of mesogenic moieties (typically 50 \AA in diameter) arranged into strata in which the plane of the layer is tilted with respect to the axis of the mesogene by an angle approximately equal to the azimuthal angle of the sharp

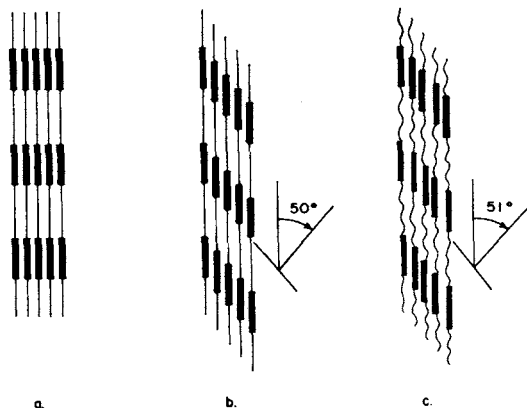


Fig. 7. Schematic of chain packing in oriented DDA-9: (a) magnetically oriented fiber crystallite, (b) extrusion-oriented fiber crystallite, (c) magnetically oriented (quenched) nematic "cybotactic" cluster of chains.

low-angle reflections. The repeat distance along the chain direction is $16.5 \text{ \AA} / \cos 51^\circ = 26 \text{ \AA}$, which is within the experimental error of the 25.2 \AA value for a fully extended repeat unit.

CONCLUSION

Properties of linear polyesters based on azoxybenzene moieties with unambiguous nematic and cholesteric phases have been described. Structure broadening by substitution of methyl groups in the 2,2' and 3,3' positions of the mesogenic core produces quite soluble polymers which can be investigated in the melt without risk of thermal decomposition. Investigation of dilute solutions of the series-9 polymers gives a viscosity law with an exponent of 0.76, indicating well-solvated, coiled conformations. This is confirmed by magnetic birefringence studies,¹⁴ which also show randomly coiled conformations in dilute solution and in the isotropic melt of some mesogenic polyesters.^{14,18} This brings up the question of the conformation of the flexible spacers in the nematic melt of these polymers. According to Roviello and Sirigu,⁵ the flexible spacer is in a random conformation and can be considered as a "solvent" in a lyotropic liquid-crystalline system. Our experimental data do not support this type of model for the systems described here. In a homologous series of low-molecular-weight 4,4'-*n*-alkoxyazoxybenzenes¹⁵ and 4,4'-*n*-alkylazoxybenzenes²³ calorimetric data show an increase in isotropization entropy ΔS_{NI} with increasing length of the terminal group. The systematic increase in ΔS_{NI} shown in Table II for increasing spacer length suggests a nonrandom conformation of the spacer chain with a degree of order superior to that of low-molecular-weight analogs. This interpretation is consistent with the results of our preliminary proton NMR investigation of a macroscopically aligned nematic melt of DDA-9.^{16,21} It is also consistent with proton spin-lattice relaxation time measurements in the nematic phase of 4,4'-dihexyloxyazoxybenzene, which show that the aliphatic chains are dynamically coupled with the nematic director.²⁴ Our x-ray data also support the extended-chain model in the nematic phase, especially data obtained with the quenched nematic glass.

The drastic influence of the position of the ester group on the stability of the mesophase (Table III) can be interpreted by assuming that stability of the polymer mesophase will be enhanced if randomness (probability of *gauche* conformation) in the spacer is decreased. If we consider the $-\text{O}-\text{CO}-$ $(\text{CH}_2)_n-\text{CO}-\text{O}-$ sequence, which is the bridging group in the 8, 9, and 14 series, and assume a dihedral angle of ca. 55° between the plane of the ester group and the aromatic plane,²⁵ we can represent the monomer sequence in the macromolecule in the nematic state using a model in which two consecutive mesogenic units are roughly parallel and colinear without significant distortion of the bridging group from a *trans* conformation. In azoxy B-10 and SUB-10, on the other hand, a similar model would require a significant population of *gauche* conformations with decreased chain order and decreased mesophase stability.

In conclusion, our data support a picture of an extended repeat unit in the nematic state.

This work was supported by the National Science Foundation Polymer Program under Grant DMR-7925059. The authors would like to express their thanks to Dr. Won-Ho Sohn for the preparation of the azoxy B-10 polymer and Mr. C. Chen for the extrusion of the DDA-9 fiber.

References

1. A. Blumstein, K. N. Sivaramakrishnan, S. B. Clough, and R. B. Blumstein, *Polym. Prepr. Am. Chem. Soc. Div. Polym. Chem.*, **19**, 2, 190 (1978); *Mol. Cryst. Liq. Cryst. Lett.*, **49**, 255 (1979); *Polymer*, **23**, 47 (1982).
2. S. Vilasagar and A. Blumstein, *Mol. Cryst. Liq. Cryst.*, **56**, 263-269 (1980).
3. A. Blumstein and S. Vilasagar, *Mol. Cryst. Liq. Cryst. Lett.*, **72**, 1 (1981).
4. A. Roviello and A. Sirigu, *Eur. Polym. J.*, **15**, 61 (1979).
5. A. Roviello and A. Sirigu, *Makromol. Chem.*, **181**, 1799 (1980).
6. J. I. Jin, S. Antoun, C. Ober, and R. W. Lenz, *Br. Polym. J.*, **12**, 132 (1980).
7. B. Millaud, A. Thierry, C. Stratielle, and A. Skoulios, *Mol. Cryst. Liq. Cryst.*, **49**, 299 (1979).
8. L. Strzelecki and D. van Luyen, *Eur. Polym. J.*, **16**, 299, 303, 307 (1980).
9. L. Liebert, L. Strzelecki, D. van Luyen, and A. M. Levelut, *Eur. Polym. J.*, **17**, 71 (1981).
10. B. Fayolle, C. Noel, and J. Billard, *J. Phys. Paris, Coll. 3, Suppl.* **40**, 485 (1979).
11. N. J. Leonard and J. W. Curry, *J. Org. Chem.*, **17**, 1071 (1952).
12. R. A. Raphael and E. Vogel, *J. Chem. Soc. Perkins Trans. 2*, **2**, 1958 (1952).
13. *Organic Synthesis*, Vol. II, p. 16 (collective).
14. A. Blumstein, G. Maret, and S. Vilasagar, *Macromolecules*, **14**, 1543 (1981).
15. M. Arnold, *Z. Phys. Chem. (Leipzig)*, **226**, 146 (1964).
16. F. Volino, A. F. Martins, R. B. Blumstein, and A. Blumstein, *C. R. Acad. Sci.*, **292**, II, 829 (1981); *J. Physique (lettres)*, **42**, L-305 (1981).
17. H. Finkelmann, J. Kaldehoff, and H. Ringsdorf, *Angew. Chem. Int. Ed. Engl.*, **17**, 935 (1978).
18. G. Maret, A. Blumstein, and S. Vilasagar, *Polym. Prepr. Am. Chem. Soc. Div. Polym. Sci.*, **22**, 1, 246 (1981).
19. I. G. Chistyakov and W. M. Chaikovsky, *Mol. Cryst. Liq. Cryst.*, **7**, 269 (1969).
20. A. deVries, *Mol. Cryst. Liq. Cryst.*, **10**, 219 (1970).
21. G. Maret, F. Volino, R. B. Blumstein, A. F. Martins, and A. Blumstein, Proceedings of the IUPAC Macromolecular Symposium, Strasbourg, **11**, 829 (1981).
22. G. Maret and A. Blumstein, *Mol. Cryst. Liq. Cryst.*, to appear.
23. J. van der Veen, W. H. de Jeu, J. W. M. Wanninkhof, and C. A. M. Tienhoven, *J. Phys. Chem.*, **77**, 2153 (1973).
24. A. F. Martins, J. B. Bonfim, and A. M. Giroud-Godquin, *Prot. Phys.*, **11**, 159 (1980).
25. J. P. Hummell and P. J. Flory, *Macromolecules*, **13**, 979 (1980).

Received June 30, 1981

Accepted October 13, 1981